STUDY ON MECHANICAL BEHAVIOR OF DOWEL BAR IN TRANSVERSE JOINT OF CONCRETE PAVEMENT

Tatsuo Nishizawa
Associate Professor, Ishikawa National College of Technology
Tsubata Ishikawa 929-0392 JAPAN
TEL: +81-76-288-8167, FAX:+81-76-288-8171
E-mail: nishi@ishikawa-nct.ac.jp

Masashi Koyanagawa
Associate Professor, Tokyo University of Agriculture
1-1-1 Sakuragaoka, Setagaya-ku, Tokyo, 156-8502 JAPAN
TEL: +81-3-5477-2344, FAX: +81-3-5477-2620
E-mail: elric@nodai.ac.jp

Yasushi Takeuchi
Lecturer, Tokyo University of Agriculture
1-1-1 Sakuragaoka, Setagaya-ku, Tokyo, 156-8502 JAPAN
TEL: +81-3-5477-2342, FAX: +81-3-5477-2620
E-mail: bamboo@nodai.ac.jp

Makoto Kimura
Pavement Division, Public Works Research Institute, Ministry of Construction
1 Asahi Tsukuba 305-0804 JAPAN
TEL: +81-298-64-4607, FAX: +81-298-0178
E-mail: kimura@pwri.go.jp

ABSTRACT
The objective of this study is to develop a mechanical design method for doweled joint. In order to investigate the mechanical behavior of dowel bar, a mechanical model for dowel bar in transverse joint of concrete pavement based on three dimensional finite element method PAVE3D was developed. In the model, a dowel bar is divided into two segments embedded in concrete and a segment between them and these segments are modeled by the solution of the beam on elastic foundation and the three dimensional beam element, respectively. The model was verified by comparing the predicted strains in concrete slab and dowel bar with the experimental data which were obtained from loading tests conducted on a model pavement and an actual pavement. The effects of transverse joint structure and subbase stiffness on the stresses in dowel bar and concrete slab were investigated based on numerical simulations with PAVE3D.

INTRODUCTION

Transverse joint in concrete pavement is one of structural weak points because of the discontinuity and supposed to be a critical area in the structural design of concrete pavements. In the transverse joint, dowel bars are used to enhance load transfer across the joint. Geometry and spacing of the dowel bars are determined empirically in the manual in Japan [1]. A condition survey of concrete pavements in Japan showed that many concrete pavements in heavy duty roads have suffered from longitudinal cracks initiating at transverse joints in wheel paths [2]. Other study showed that some dowel bars broke down at joint opening of transverse joint [3]. These facts are suggesting that the current design of dowel bar at the transverse joint might be inappropriate. Therefore, rational design method for the doweled joint based on a mechanical analysis is required.

The finite element models based on the plate theory have been employed to analyze the mechanical behaviors concrete slabs at transverse joints, including dowel actions [4,5,6,7,8]. In these models, the dowel bar function at the joint is represented by shear spring and/or beam element. The authors have proposed a refined model for the dowel bar function, where a dowel bar is divided into a segment between concrete slabs and two segments embedded in concrete [9,10]. These segments are modeled with a beam element and local displacement elements, respectively. This model was employed by another researchers in FE analysis and its validity was confirmed [11].

Three dimensional finite element method (3DFEM) has been recognized as a powerful tool for analysis and design of pavement structures. Recently, two symposiums relating to this subject were held in U.S.A [12, 13]. 3DFEM allows pavement engineers to compute displacements and stresses not only in concrete slabs but also in subbase and subgrade where 2D slab model was not able to deal with. In 3DFEM for concrete pavement, the load transfer model across the joint is still significantly important [14,15]. In this study, we developed 3DFEM code for concrete pavement accommodating dowel bar function at transverse joint as well as an open-closure phenomenon at the interface between concrete slab and subbase. The code of 3DFEM for pavement structure developed in this study was named as PAVE3D, which consists of an FEM solver and pre-post processors. We incorporated the refined dowel model into PAVE3D and investigated the effects of geometry and spacing of dowel bar and subbase stiffness on stresses in dowel bar and concrete slab.

STRUCTURAL MODEL

3DFE Model for Pavement

Figure 1 shows a pavement structure considered in the PAVE3D. The pavement consists of elastic layers of concrete slab, subbase and subgrade, all of which are divided into solid elements. The interface between the concrete slab and the subbase is modeled with a general interface element.

Dowel bar element is included in the joint interface element.

Each layer has finite extent horizontally and the displacement in the normal direction on each edge is fixed but others are free. This boundary condition is not applied to the top layer. All displacements are fixed at the bottommost of the structure. Load is applied on the surface both vertically and horizontally as a uniformly distributed rectangular load. Temperature distribution can be specified as a linear function of z for each layer.

Solid Element

Eight node solid element as shown in Figure 2 is employed in this study. Displacements in the solid element are expressed with shape functions as follows [16]:

$$\begin{Bmatrix} u \\ v \\ z \end{Bmatrix} = \sum_{i=0}^{7} \begin{bmatrix} N_i & 0 & 0 \\ 0 & N_i & 0 \\ 0 & 0 & N_i \end{bmatrix} \begin{Bmatrix} u_i \\ v_i \\ w_i \end{Bmatrix} \qquad (1)$$

where,

$u,\ v,\ w$ = displacements in x, y and z directions, respectively, within an element,

$u_i,\ v_i,\ w_i$ = displacements in x, y and z directions, respectively, at a node, i, and

$N_i = \frac{1}{8}(1+\xi_i\xi)(1+\eta_i\eta)(1+\zeta_i\zeta)$.

Interface Element

In order to deal with bounding condition at the interface between concrete slab and subbase and aggregate interlocking at crack or joint, we developed a general interface element as shown in Figure 3. The interface element consists of two planes: Plane 0 and Plane 1. It is assumed that stresses proportional to the differentials in the displacements between the planes are transferred, which can be expressed as:

$$\begin{Bmatrix} \Delta f_{x'} \\ \Delta f_{y'} \\ \Delta f_{z'} \end{Bmatrix} = \begin{bmatrix} k_{x'} & 0 & 0 \\ 0 & k_{y'} & 0 \\ 0 & 0 & k_{z'} \end{bmatrix} \begin{Bmatrix} \Delta u' \\ \Delta v' \\ \Delta w' \end{Bmatrix} \quad or \quad \{\Delta \mathbf{f}'\} = [\mathbf{k}']\{\Delta \mathbf{d}'\} \qquad (2)$$

where

$f_{x'},\ f_{y'},\ f_{z'}$ = stresses in x’, y’ and z’ directions, respectively, within an plane,

$u',\ v',\ w'$ = displacements in x’, y’ and z’ directions, respectively, within an element, and

$k_{x'},\ k_{y'},\ k_{z'}$ = spring coefficients in x’, y’ and z’ directions, respectively.

Δ indicates the differential between Plane 0 and Plane 1. Using Equation (2) and applying the principle of virtual work to the element, the stiffness matrix can be obtained [17].

Spring Coefficients

In concrete pavement, portions of the bottom surface of concrete slab may separate from the top surface of subbase, if curling deformation due to temperature gradient in concrete slab occurs. In order to take into account this phenomenon, the spring coefficients of the interface element are assumed to be a function of displacement differential Δu as follows:

$$k = \begin{cases} k & \Delta u < 0 \\ \dfrac{k}{2}\left\{\cos\left(\dfrac{\Delta u \pi}{\Delta_0}\right) + 1.0\right\} & 0 \le \Delta u \le \Delta_0 \\ 0 & \Delta_0 < \Delta u \end{cases} \tag{3}$$

If the spring coefficients are rapidly changed with the displacements, reasonable converged solutions will not be obtained. Therefore, a transition range ($0 \le \Delta u \le \Delta_0$) is introduced in Equation (3). In this study, the value of Δ_0 is determined to be 0.0001mm from some trial calculations. If the interface element is used for modeling a crack, $k_{x'}$ and $k_{y'}$ represent shear and torsion transfer, and $k_{z'}$ represents moment and axial load transfer across the crack.

Non Linear Analysis

Global stiffness equation for 3DFEM with the solid and interface elements can be as follows:

$$(\mathbf{K}_s + \mathbf{K}_j) \cdot \mathbf{d} = \mathbf{f}_p + \mathbf{f}_v + \mathbf{f}_t \tag{4}$$

where

$\mathbf{K}_s$: stiffness matrix of 8 node solid element,

$\mathbf{K}_j$: stiffness matrix of interface element,

$\mathbf{d}$: displacement vector,

$\mathbf{f}_p$: external load vector,

$\mathbf{f}_v$: self weight load vector, and

$\mathbf{f}_t$: temperature load vector.

If the stiffness matrix of the interface element is a function of displacement, Equation (4) becomes nonlinear. We solve the equation with the Newton-Raphson method. If displacement vector at (i-1) iteration, $\mathbf{d}^{i-1}$, is known, residual forces of Equation (4) can be computed by:

$$\Delta \mathbf{r} = \mathbf{f}_p + \mathbf{f}_v + \mathbf{f}_t - (\mathbf{K}_s + \mathbf{K}_j) \cdot \mathbf{d}^{i-1} \tag{5}$$

The correction vector for the displacement, $\Delta \mathbf{d}^{i-1}$, is estimated by solving the following equation:

$$\Delta \mathbf{r} = (\mathbf{K}_s + \mathbf{K}_j) \cdot \Delta \mathbf{d}^{i-1} \tag{6}$$

Then, new displacement vector at next iteration can be obtained by $\mathbf{d}^i = \mathbf{d}^{i-1} + \Delta \mathbf{d}^{i-1}$. This process is repeated until a level of convergence is reached.

DOWEL BAR MODEL

Basic Concept

Dowel bar is divided into three segments; a segment between slabs and two segments embedded in concrete as shown in Figure 4. The segment between slabs is represented with a beam element which is connected to two solid elements (elements P and Q) at both nodes, because there is no support of the surrounding concrete for the segment. These nodes are located within the elements and defined as inner nodes: p and q, as shown in Figure 5. Displacements at the inner node p can be expressed with nodal the displacements of Element P as:

$$\begin{Bmatrix} u' \\ v' \\ w' \\ \theta_{x'} \\ \theta_{y'} \\ \theta_{z'} \end{Bmatrix}^p = \sum_{i=0}^{7} \begin{bmatrix} N_i & 0 & 0 \\ 0 & N_i & 0 \\ 0 & 0 & N_i \\ 0 & -\frac{\partial N_i}{\partial z'} & 0 \\ \frac{\partial N_i}{\partial z'} & 0 & 0 \\ 0 & 0 & 0 \end{bmatrix}^p \cdot \begin{Bmatrix} u_i' \\ v_i' \\ w_i' \end{Bmatrix}^P \quad or \quad \{d^p\} = [N_i] \cdot \{d^P\} \tag{7}$$

where

$\theta_{x'}$, $\theta_{y'}$, $\theta_{z'}$ = rotations for x’, y’, and z’ axes, respectively.

Superscripts, p and P, indicate components relating to the inner node p and Element P, respectively.

The inner node p moves after the concrete slab deforms. The position of the node p after the deformation is not identical to the original position in Element P, because of local deformation of the surrounding concrete. This situation is illustrated in figure 5(b). The local deformation is represented with a local element inserted between the nodes p and p’. The stiffness of the local element is expressed with the solution of the beam on elastic foundation as follows:

$$\begin{Bmatrix} \Delta v' \\ \Delta \theta_{x'} \end{Bmatrix} = a_0 \begin{bmatrix} a_1 & -a_2 \\ -a_2 & a_3 \end{bmatrix} \cdot \begin{Bmatrix} \Delta f_{y'} \\ \Delta m_{x'} \end{Bmatrix} \tag{8}$$

in y’-z’ plane, where

$$a_0 = \frac{2\beta^2}{k(S^2 - s^2)},\ a_1 = \frac{1}{\beta}(SC - sc),\ a_2 = (S^2 + s^2),\ a_3 = 2\beta(SC + sc),\ \beta = \sqrt[4]{\frac{K_c \phi}{4E_d I_d}}$$

K_c = interaction spring coefficient of surrounding concrete,

ϕ = diameter of dowel bar,

$E_d I_d$ = bending rigidity of dowel bar,

$s = \sin(\beta L),\ c = \cos(\beta L),\ S = \sinh(\beta L),\ C = \cosh(\beta L),$

L = embedded length of dowel bar,

$f_{y'}$ = shear force in y’ direction, and

$m_{x'}$ = moment for x’ axis.

In z'-x' plane, it becomes:

$$\begin{Bmatrix} \Delta u' \\ \Delta\theta_{y'} \end{Bmatrix} = a_0 \begin{bmatrix} a_1 & a_2 \\ a_2 & a_3 \end{bmatrix} \cdot \begin{Bmatrix} \Delta f_{x'} \\ \Delta m_{y'} \end{Bmatrix} \tag{9}$$

where

$f_{x'}$ = shear force in x' direction, and

$m_{y'}$ = moment for y' axis.

Combining Equations (8) and (9), one can obtain:

$$\{\Delta f\} = \lfloor A^P \rfloor \{\Delta d\} \tag{10}$$

where

$\{\Delta f\} = \{f^p\} - \{f^{p'}\}$,

$\{\Delta d\} = \{d^p\} - \{d^{p'}\}$,

$\{f\} = \{f_{x'} \;\; f_{y'} \;\; f_{z'} \;\; m_{x'} \;\; m_{y'} \;\; m_{z'}\}^t$ and

$\{d\} = \{u' \; v' \;\; w' \;\; \theta_{x'} \;\; \theta_{y'} \;\; \theta_{z'}\}^t$.

$\lfloor A^P \rfloor$ is a matrix of 6 by 6 and its non-zero components are:

$$A^P_{00} = A^P_{11} = a_4 a_3,\; A^P_{33} = A^P_{44} = a_4 a_1,\; A^P_{04} = -A^P_{13} = -a_4 a_2,\; a_4 = \frac{2\beta^2 E_s I_s}{C^2 + c^2}$$

Applying the theory of virtual work to the local element between the nodes, p and p', one obtains the following relationship:

$$\begin{Bmatrix} f^p \\ f^{p'} \end{Bmatrix} = \begin{bmatrix} A^P & -A^P \\ -A^P & A^P \end{bmatrix} \cdot \begin{Bmatrix} d^p \\ d^{p'} \end{Bmatrix} \tag{11}$$

For the local element between the nodes, q and q', it becomes:

$$\begin{Bmatrix} f^q \\ f^{q'} \end{Bmatrix} = \begin{bmatrix} A^Q & -A^Q \\ -A^Q & A^Q \end{bmatrix} \cdot \begin{Bmatrix} d^q \\ d^{q'} \end{Bmatrix} \tag{12}$$

The stiffness equation for the three dimensional beam element between the nodes, p' and q' is [18]:

$$\begin{Bmatrix} f^{p'} \\ f^{q'} \end{Bmatrix} = \begin{bmatrix} S_{00} & S_{01} \\ S_{10} & S_{11} \end{bmatrix} \cdot \begin{Bmatrix} d^{p'} \\ d^{q'} \end{Bmatrix} \tag{13}$$

Superimposing all equations mentioned above, the stiffness equation for the overall dowel bar becomes:

$$\begin{Bmatrix} f^p \\ f^{p'} \\ f^{q'} \\ f^q \end{Bmatrix} = \begin{bmatrix} A^P & -A^P & 0 & 0 \\ -A^P & A^P + S_{00} & S_{01} & 0 \\ 0 & S_{10} & A^Q + S_{11} & -A^Q \\ 0 & 0 & -A^Q & A^Q \end{bmatrix} \cdot \begin{Bmatrix} d^p \\ d^{p'} \\ d^{q'} \\ d^q \end{Bmatrix} \tag{14}$$

Considering

$$\begin{Bmatrix} f^{p'} \\ f^{q'} \end{Bmatrix} = \begin{Bmatrix} 0 \\ 0 \end{Bmatrix}, \tag{15}$$

one obtains the stiffness matrix of the dowel bar element as follows:

$$\begin{Bmatrix} f^p \\ f^q \end{Bmatrix} = \begin{bmatrix} K_{00}^d & K_{01}^d \\ K_{10}^d & K_{11}^d \end{bmatrix} \cdot \begin{Bmatrix} d^p \\ d^q \end{Bmatrix} \tag{16}$$

where

$$\begin{bmatrix} K_{00}^d & K_{01}^d \\ K_{10}^d & K_{11}^d \end{bmatrix} = \begin{bmatrix} A^P & 0 \\ 0 & A^Q \end{bmatrix} \left[\begin{bmatrix} I & 0 \\ 0 & I \end{bmatrix} - \begin{bmatrix} A^P + S_{00} & S_{01} \\ S_{10} & A^Q + S_{11} \end{bmatrix}^{-1} \begin{bmatrix} A^P & 0 \\ 0 & A^Q \end{bmatrix} \right] \tag{17}$$

and $[I]$ is an unit matrix of 6 by 6. On the other hand, if the joint width is very narrow, the beam element between the nodes, p' and q' is removed and two local elements are directly connected at a node. In this case, the stiffness matrix of the dowel bar element becomes:

$$\begin{bmatrix} K_{00}^d & K_{01}^d \\ K_{10}^d & K_{11}^d \end{bmatrix} = \begin{bmatrix} A^P & 0 \\ 0 & A^Q \end{bmatrix} \left[\begin{bmatrix} I & 0 \\ 0 & I \end{bmatrix} - \begin{bmatrix} A^P \cdot B \cdot A^P & A^P \cdot B \cdot A^Q \\ A^Q \cdot B \cdot A^P & A^Q \cdot B \cdot A^Q \end{bmatrix} \right] \tag{18}$$

where

$$[B] = \left[A^P + A^Q\right]^{-1}$$

Using Equation (7), Equations (17) and (18) can be converted to the stiffness equation expressed with displacement vectors of the solid elements, P and Q:

$$\begin{Bmatrix} f^P \\ f^Q \end{Bmatrix} = \begin{bmatrix} N^p & 0 \\ 0 & N^q \end{bmatrix}^t \cdot \begin{bmatrix} K_{00}^d & K_{01}^d \\ K_{10}^d & K_{11}^d \end{bmatrix} \cdot \begin{bmatrix} N^p & 0 \\ 0 & N^q \end{bmatrix} \cdot \begin{Bmatrix} d^P \\ d^Q \end{Bmatrix} \tag{19}$$

Since Equation (19) is formulated in the local coordinate of the interface element, it should be transferred to that in the global coordinate by using the coordinate transfer matrix.

VERIFICATION OF DOWEL BAR MODEL

Model Pavement

In order to experimentally investigate the mechanical behavior of dowel bar, a model pavement with 100mm thick concrete slab on a granular base was constructed in a laboratory as shown in Figure 6. Two types of transverse joint with 23 mm diameter and 11 mm diameter dowel bars were installed. Strains in the dowel bars produced by a vertical load applied at the transverse joint edge were measured with gauges attached on the surface of the dowel bars. The experiment was analyzed by PAVE3D. The mesh used in the analysis is shown in Figure 7. The input data for the analysis is presented in Table 1. The interaction spring coefficient, K_c , varied from 100 GN/m^3 to 400 GN/m^3 according to Yoder et al[19].

Figure 8 shows comparisons of the predicted bending strains in a dowel bar just under the load with the measured ones. In the case of 11mm diameter dowel bar, measured strain distribution was nearly symmetrical shape with respect to the center of the dowel bar, because the shear load transfer was predominant. On the other hand, in the case of 23mm diameter dowel bar, strains in the loaded side were much larger than those in the unloaded side, because contribution of the bending action of the dowel bar to the load transfer was significant in this case. Strains computed by PAVE3D showed similar tendency with the measured ones. The computed strains became larger by 25 to 30 % as K_c increased from 100GN/m^3 to 400GN/m^3.

Actual Pavement

A loading test was conducted on a concrete pavement constructed in an express highway to investigate the mechanical behavior of transverse joint in an actual situation. The Figure 9 shows a section of the pavement which has 280mm thick concrete slab on 150mm thick cement stabilized subbase. Four types of transverse joint were constructed to study the effects of diameter and spacing of dowel bar as shown in Figure 10. Strain gauges were attached on the top and bottom surfaces of third and fourth dowel bars from the longitudinal edge with an interval of 30 mm as well as on the top surface of the slab along the transverse joint edge with an interval of 200 mm. A large truck with tandem rear axle (98kN per axle) was used to apply loads at the transverse joint. The strains in the dowel bars and slabs were measured when the axle approached the joint edge. The loading test was analyzed by using the mesh as shown in Figure 11 and the input data presented in Table 2. In this analysis, K_c of 400 GN/m^3 was used.

Figure 12 shows the strain distributions in the dowel bars with strain gauges. Some of the strain gauges on the dowel bar did not work, so strains reliably measured are plotted in the figure. Although the predicted strains overestimate the measured ones, the agreement between the predicted and measured ones are fairly well from a practical point of view.

Figure 13 shows the strain distributions on the slab surface along the transverse joint. Although the predicted strains are larger than the measured ones, the tendencies of both strains are quite similar. From these results, it can be said that PVAE3D is able to predict the behaviors of dowel bars as well as concrete slabs.

MECHANICAL BEHAVIOR OF TRANSVERSE JOINT

In this chapter, effects of geometry and spacing of dowel bar and subbase rigidity on the mechanical behaviors of concrete slab and dowel bar will be investigated with PAVE3D simulations. The simulations were performed on a concrete pavement with the transverse joint of Type 3 as a reference structure. Length of dowel bar, value of K_c , width of joint opening, L_b , and subbase stiffness, E_b , varied as presented in Table3. The width of joint opening mentioned here is a length of the beam element and is not necessarily the actual opening of the slabs. If the length is greater than the actual opening, the inner nodes are located not on the surface of the solid elements but within them, which means that the support of concrete at the potion near the center of the dowel bar is lost.

Stress of Dowel Bar

Figure 14 shows the distributions of the maximum bending stress in the dowel bars along the joint edge. As the diameter of the dowel bar increases from 28 mm to 32 mm, the maximum stress decreases by about 25%. On the other hand, 20% stress reduction is obtained by narrowing the dowel spacing from 400 mm to 300 mm.

Figure 15 shows the effect of K_c on the bending stress in the dowel bars. As K_c increases, the range where bending stress occurs becomes narrow and the magnitude of the maximum stress increases. Change of the dowel bar length from 700 mm (solid line in Figure 15(a)) to 500 mm (circle marks) has no effect on the bending stress. From Figure 15(b), it is found that, if K_c = 400 GN/m^3, the bending stress of the dowel bar just under the tire is greater than those with K_c = 100 GN/m^3 and the bending stresses in other dowel bars between the tires are smaller. So, if the restraint of concrete to the dowel bars is strong, the stresses in the dowel bars under the tires are large but those between the tires are relatively small.

Figure 16 shows the effect of L_b on the bending stress in the dowel bars. Increase of the length from 20 mm to 60 mm increases the bending stresses of all dowel bars by about 40%. Therefore, if the concrete around the dowel bar near the joint opening weakens and loses the ability to support the dowel there, the stress of the dowel bar would significantly increase.

Figure 17 shows the effect of E_b on the stress of the dowel bar. E_b varied from 500 MPa for a granular subbase to 10000 MPa for a lean concrete subbase. Increasing E_b decreases the bending stresses in all dowel bars by about 20%.

Stresses in Concrete Slabs

In this section, the bending stresses at the bottom of the concrete slab and the transfer efficiency across the transverse joint will be discussed.

Figure 18 shows stress distributions along the transverse joint edge in loaded and unloaded slabs to compare the stresses among the joint types. Naturally, the stresses in the loaded slab under the tires are larger than those in the other part of the slab. In the unloaded slab, relatively large stress is observed between the tires, because the load is transferred by several dowel bars in a wide range. From Figures 18(a) and (b), it can be said that increasing the dowel diameter from 28mm to 32mm has very little effect on concrete stress. From Figure 18(c), we can not see any difference in the stress between the two dowel spacings of 400 mm and 300 mm. Therefore, the joint type considered in this experiment has not significant effect on the concrete stress.

In this study, the load transfer efficiency expressed in deflection or stress is defined as follows:

$$e_{ff} = \frac{2s_2}{s_1 + s_2} \times 100 \qquad (20)$$

where

e_{ff} = load transfer efficiency(%)

s_1, s_2 = responses of the loaded and unloaded slabs, respectively.

Figure 19 shows the effect of K_c on e_{ff}. An increase in K_c decreases the stress in the loaded slab and increases the stress in the unloaded slab, leading to higher e_{ff} in stress, while the effect of K_c on deflection is very little.

Figure 20 shows the effect of L_b on e_{ff}. In the range of L_b less than 40mm, the effect seems to be very little. Increase in L_b over 60mm increases the stress and deflection in the loaded slab and decreases these in unloaded slab, leading to the lower e_{ff}. In general practices, the width of joint opening is 10 to 20 mm. In this range, there might be no impact on the concrete stresses, which means the effectiveness of the dowel bar. However, if the concrete around the dowel bar becomes weak after the repeated loading action, the support of the concrete to the dowel bar will be lost and the length of unsupported part of the dowel bar may increase to more than 40mm, leading to higher bending stress in the concrete slabs.

Figure 21 shows the effect of E_b on the concrete stress. Increase in E_b decreases both the deflections and stresses in the loaded and unloaded slabs, though the increase has little effect on e_{ff}. Therefore, strengthening the subbase might be a good measure to increase the structural capacity of the whole pavement system for the traffic loading.

CONCLUSION

In this study, a mechanical model for dowel bar in transverse joint of concrete pavement based on three dimensional finite element method was developed. In the model, a dowel bar is divided into two segments embedded in concrete and a segment between them and these segments are modeled by the solution of the beam on elastic foundation and the three dimensional beam element, respectively. This dowel bar element was formulated for a 3DFEM code: PAVE3D, which allows one to compute the displacements and stresses in dowel bar as well as in concrete slab, subbase and subgrade, taking into account the geometry and spacing of dowel bar.

The model was verified by comparing the predicted strains in concrete slab and dowel bars with the experimental data that were obtained from loading tests conducted on a model pavement and an actual pavement. The comparison showed a fairly good agreement and confirmed the validity of PAVE3D.

The effects of transverse joint structure on the stresses in dowel bar and concrete slab were investigated based on numerical simulations with PAVE3D. The results showed that the geometry and spacing of dowel bar have great effect on the stress in dowel bar but the effect on the stresses on the concrete slab is relatively small. It was also found that increasing the subbase rigidity decreases the stresses in both dowel bar and concrete slab. Therefore, strengthening the subbase might be a good measure to enhance the structural capacity of concrete pavement system.

REFERENCES

1. *Manual for Portland Cement Concrete Pavement*, Japan Road Association, 1981.
2. Fukuda, T., Koyanagawa, M., and Murai, S., Condition Survey of Concrete Pavements and Its Evaluation, *Proceedings of 3rd International Conference on Concrete Pavement Design and Rehabilitation*, Purdue University, pp.519-523, 1985.
3. Iijima, T., and Kubota, K., Evaluation of Serviceability of Test Pavement in Yaita Bypass, *Proc. of JSCE*, No. 388/V-4, pp.65-74, 1980.
4. Tabatabaie, A.M., and Barenberg, E.J., Finite Element Analysis of Jointed or Cracked Concrete Pavements, *Transportation Research Record 671*, Transportation Research Board, pp.11-17, 1978.
5. Huang, Y.H., and Chou, Y.T., Discussion on Finite Element Analysis of Jointed or Cracked Pavements, *Transportation Research Record 671*, Transportation Research Board, pp.17-18, 1978.
6. Tayabiji, S.D., and Colley, B.E., Analysis of Jointed Concrete Pavements, *FHWA-RD-86-041*, Turner-Fairbanks Highway Res. Ctr., McLean, Va., 1986.
7. Ioannides, A.M., Analysis of Slab-on-grade for a Variety of Loading and Support Conditions, PhD thesis, University of Illinois, Urbana, Ill., 1984.
8. Fukute, T., Hachiya, Y., and Yamazaki H., Load Transfer Function across Joint in Concrete Pavement, *Report of Port Harbor Research Institute*, Ministry of Transportation, Vol.21, No.2, pp.207-236, 1982.
9. Nishizawa, T., Fukuda, T., and Matsuno, S., Analysis of Mechanical Behavior of Transverse Joint in Concrete Pavement, *Proc. of JSCE*, No.378/V-6, pp.185-193, 1987.
10. Nishizawa, T., Fukuda, T., and Matsuno, S., A Refined Model of Doweled Joints for Concrete Pavement Using FEM, *Proceedings of 4th International Conference on Concrete Pavement Design and Rehabilitation*, Purdue University, pp. 735-745, 1989.
11. Guo, H., Sherwood, J.S., and Snyder, M.B., Component Dowel-Bar Model for Load Transfer Systems in PCC Pavements, *Journal of Transportation Engineering*, ASCE, Vol. 121, No. 3, pp.289-298, 1995.
12. *Proceedings of National Symposium on 3D Finite Element Modeling for Pavement Analysis, Design, and Research*, Charleston, West Virginia, 1998.
13. *Proceedings of 2nd International Symposium on 3D Finite Element for Pavement Analysis, Design, and Research*, Charleston, West Virginia, 2000.
14. Shoukry, S.N., and William, G., 3D FEM Analysis of Load Transfer Efficiency, *Proceedings of National Symposium on 3D Finite Element Modeling for Pavement Analysis, Design, and Research*, Charleston, West Virginia, pp.40-50, 1998.
15. Davids, W.G., and Mahoney, J.P., Experimental Verification of Rigid Pavement Joint Load Transfer Modeling with EverFE, *Transportation Research Record 1684*, Transportation Research Board, pp. 81-89, 1998.
16. Zienkievicz, O.C., *The Finite Element Method*, Third Edition, McGraw-Hill, Inc., 1977.
17. Nishizawa, T., Development of 3D FEM Program Package for Structural Analysis of Pavement System, *Journal of Pavement Engineering*, JSCE, Vol.5, 2000. (http://www.plan.civil.tohoku.ac.jp/ pave/ hoso-ml/ download.html)
18. Przemienieki, J.K., *Theory of Matrix Structural Analysis*, McCraw-Hill, Inc., p.79, 1968.
19. Yorder, E.J., and Witczak, M.W., *Principle of Pavement Design*, Second Edition, Jhon Wiley and Sons, Inc., New York, p.99, 1975.

Table 1 Input Data for the Analysis of Loading Test on Model Pavement

Items [Symbol]	Values
Elastic Modulus of Concrete [E_c]	24000 MPa
Poisson Ration of Concrete [μ_c]	0.2
Thickness of Concrete Slab [h_c]	100 mm
Elastic Modulus of Foundation [E_b]	50 MPa
Poisson Ration of Foundation [μ_b]	0.35
Thickness of Foundation [h_b]	1200 mm
Diameter of Dowel Bar [ϕ]	11 mm and 23 mm
Length of Dowel Bar [L_d]	500 mm
Elastic Modulus of Dowel Bar [E_d]	210000 MPa
Poisson Ratio of Dowel Bar [μ_d]	0.3
Interaction Spring Constant between Dowel Bar and Concrete [K_c]	100, 200, and 400 GN/m^3

Table 2 Input Data for the Analysis of Loading Test on Actual Pavement

Items [Symbol]	Values
Elastic Modulus of Concrete [E_c]	30000 MPa
Poisson Ration of Concrete [μ_c]	0.15
Thickness of Concrete Slab [h_c]	280 mm
Elastic Modulus of Subbase [E_b]	1000 MPa
Poisson Ration of Subbase [μ_b]	0.35
Thickness of Subbase [h_b]	150 mm
Elastic Modulus of Subbase[E_g]	30 Mpa
Poisson Ration of Subbase [μ_g]	0.35
Thickness of Subbase [h_g]	2600 mm
Diameter of Dowel Bar [ϕ]	28 mm and 32 mm
Length of Dowel Bar [L_d]	700 mm
Elastic Modulus of Dowel Bar [E_d]	210000 MPa
Poisson Ratio of Dowel Bar [μ_d]	0.3
Interaction Spring Constant between Dowel Bar and Concrete [K_c]	400 GN/m^3

Table 3 Variations of Parameters for Simulation

Items [Symbol]	Values
Elastic Modulus of Subbase [E_b]	500, 1000, 10000 MPa
Diameter of Dowel Bar [ϕ]	28 mm and 32 mm
Length of Unsupported Dowel Bar [L_b]	20, 40, and 60 mm

Length of Dowel Bar [L_d]	500, and 700 mm
Interaction Spring Constant between Dowel Bar and Concrete [K_c]	100, 200, and 400 GN/m^3

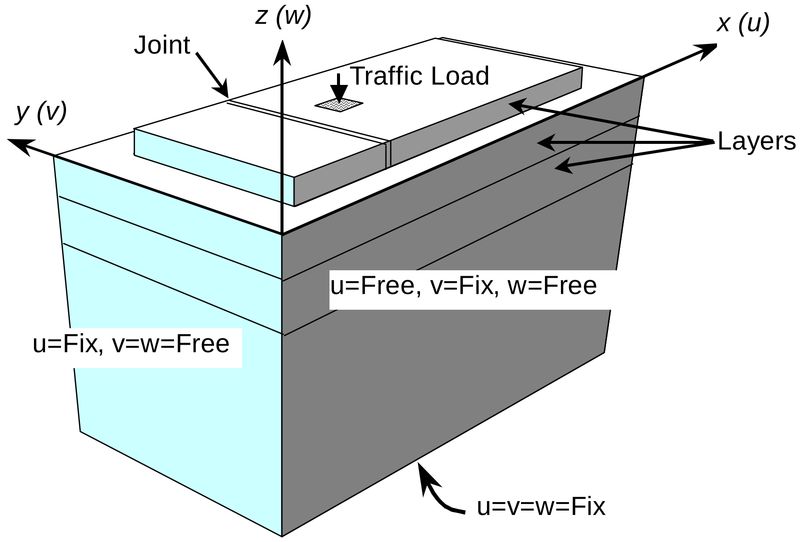

Figure 1 Structural Model for Pavement

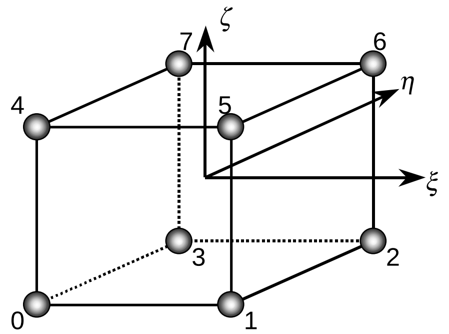

Figure 2 Eight Node Solid Element

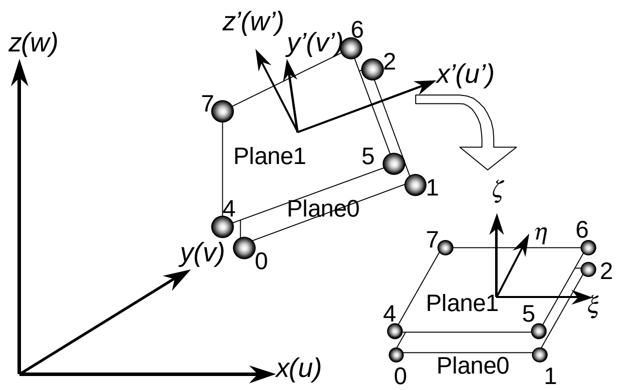

Figure 3 General Interface Element

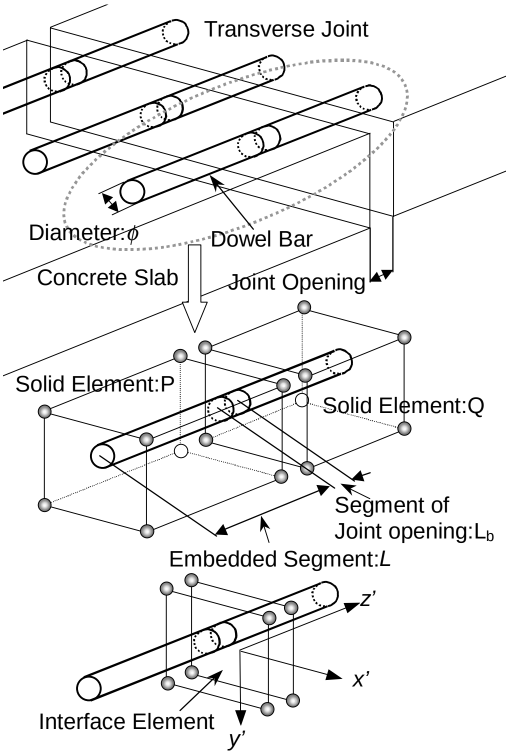

Figure 4 Dowel Bar Element

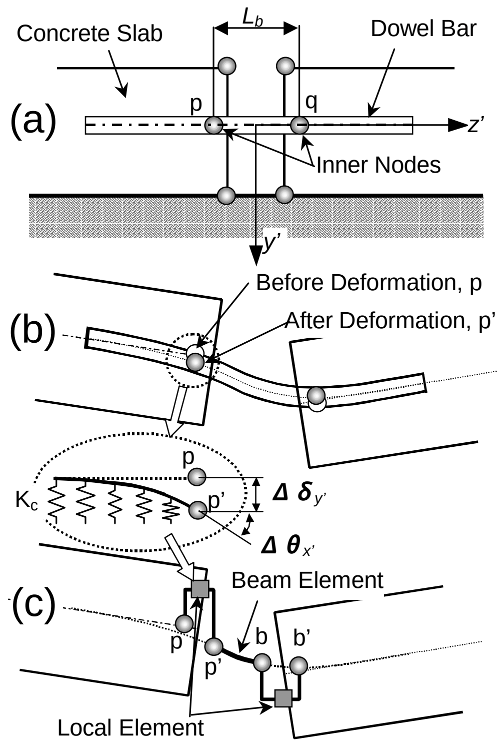

Figure 5 Displacement of Dowel Bar Element

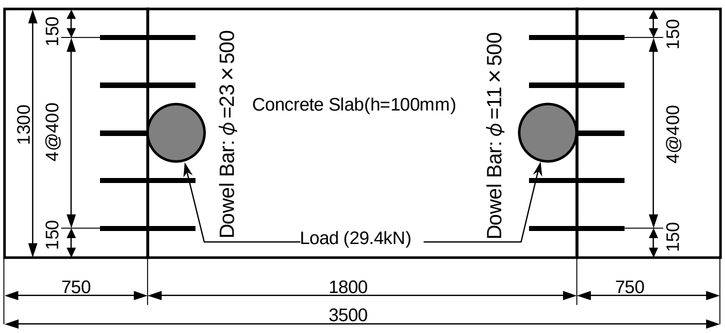

Figure 6 Overview of Model Pavement

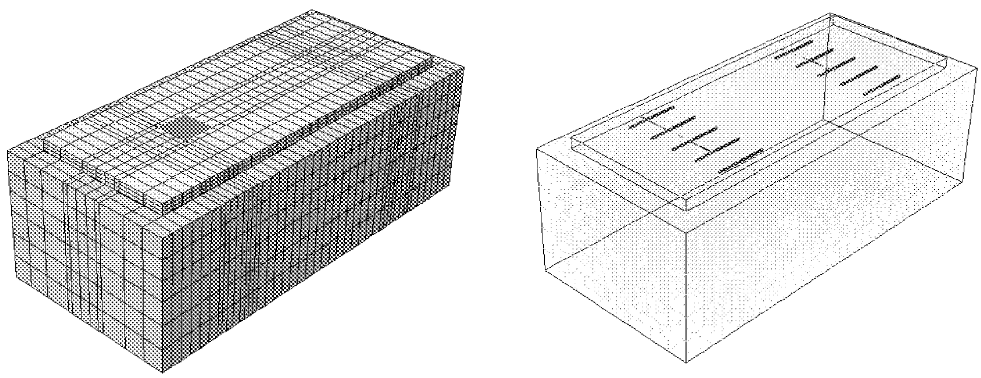

Figure 7 Mesh and Dowel Bar Arrangement for Analysis of Model Pavement

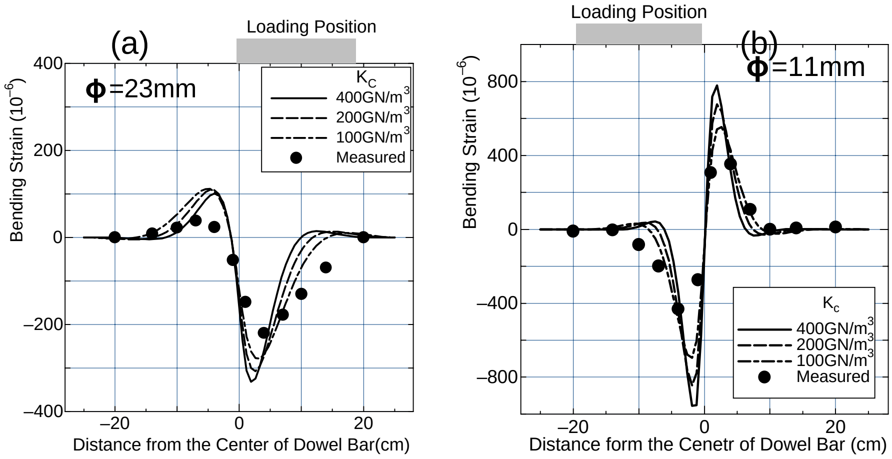

Figure 8 Strain Distributions in Dowel Bars; (a) ϕ=23mm;(b) ϕ =11mm.

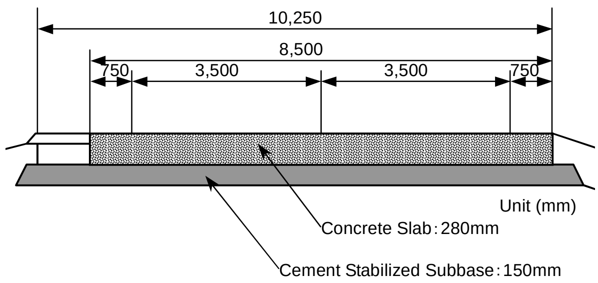

Figure 9 Overview of Actual Pavement

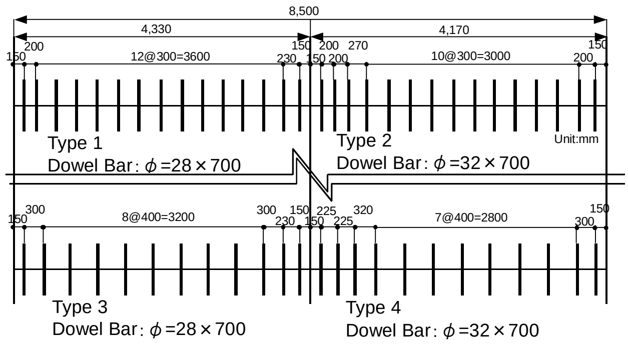

Figure10 Arrangement of Dowel Bars in Transverse Joints

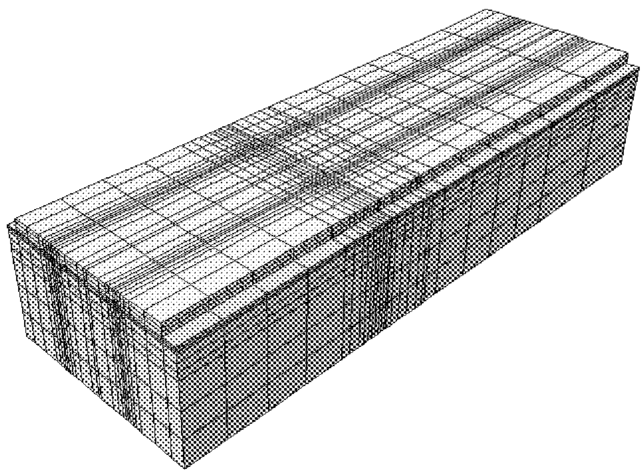

Figure 11 Mesh for Analysis of Actual Pavement

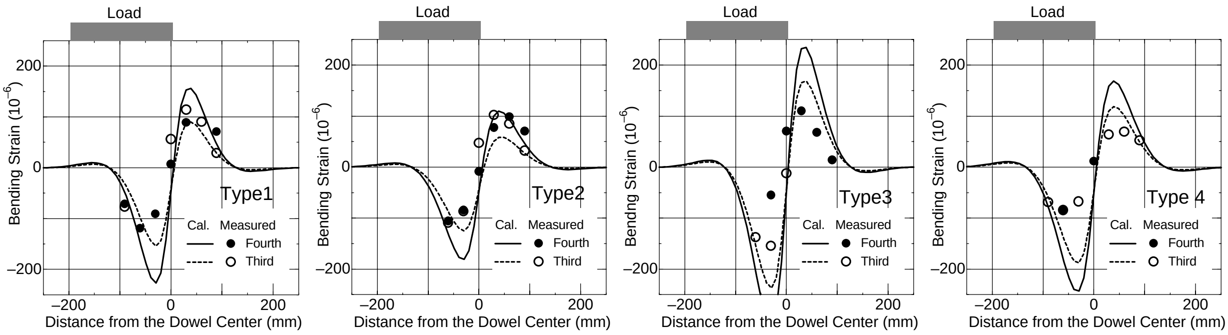

Figure 12 Strain Distributions in Dowel Bars in Actual Pavement

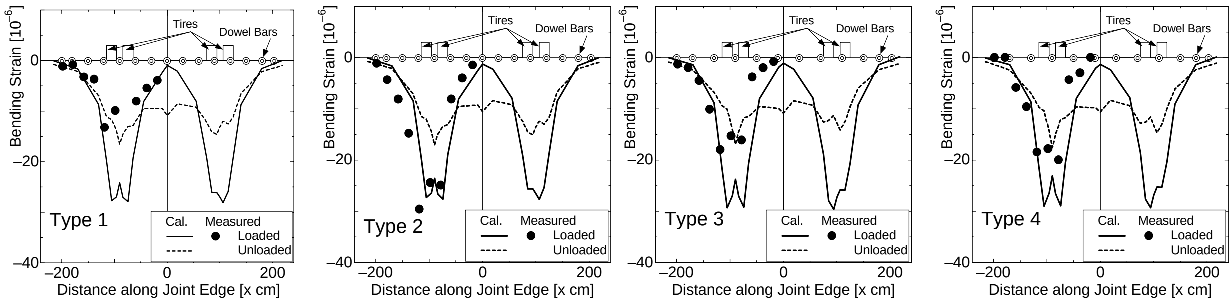

Figure 13 Strain Distributions in Concrete Slabs in Actual Pavement

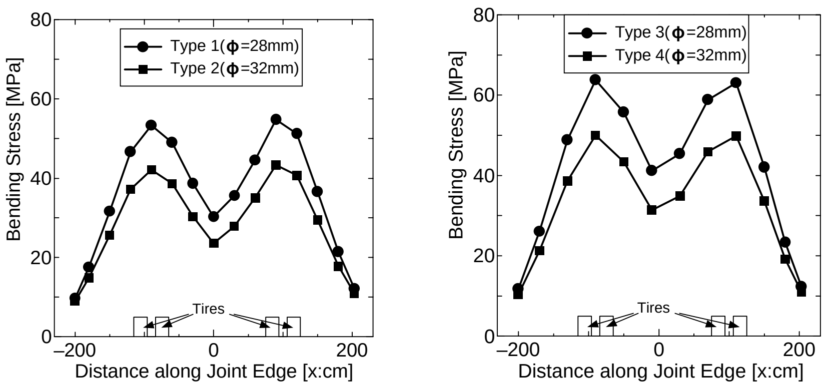

Figure 14 Maximum Bending Stresses of Dowel Bars along Joint Edge

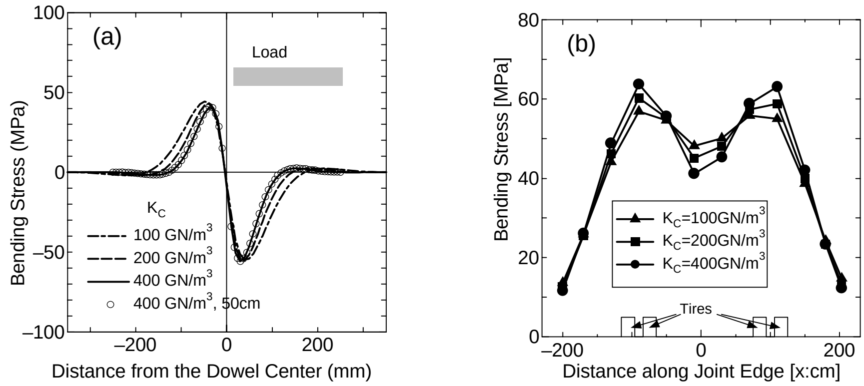

Figure 15 Effect of K_c on Bending Stress of Dowel Bar; (a) Stress Distribution in a Dowel Bar; (b) Stresses along Joint Edge.

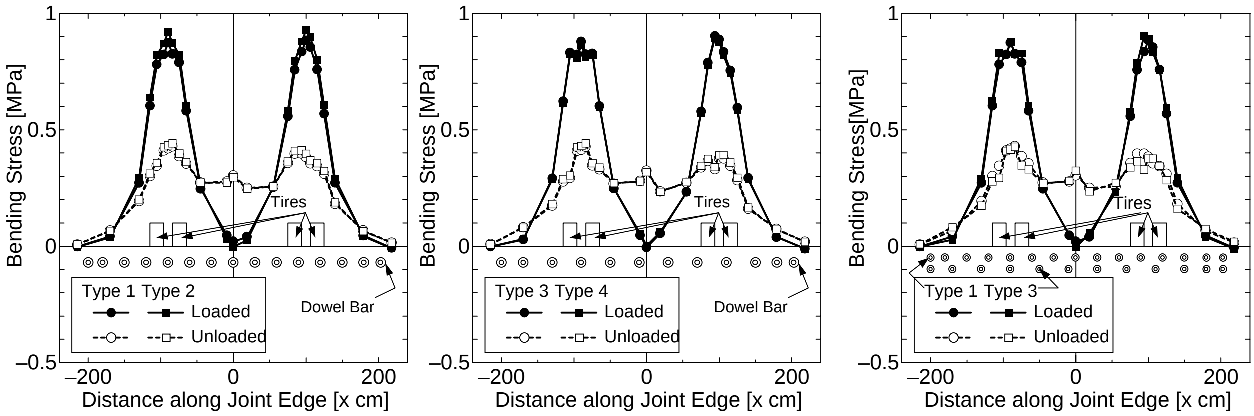

Figure 18 Bending Stress Distributions in Concrete Slab along Transverse Joint Edge

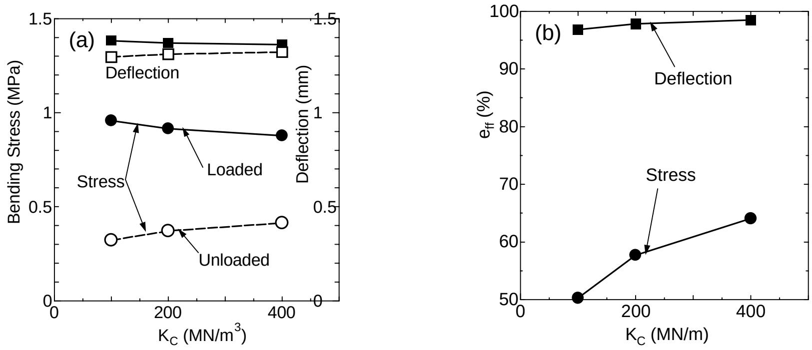

Figure 19 Effect of K_c on (a) Stress and Deflection and (b) Load Transfer Efficiencies.

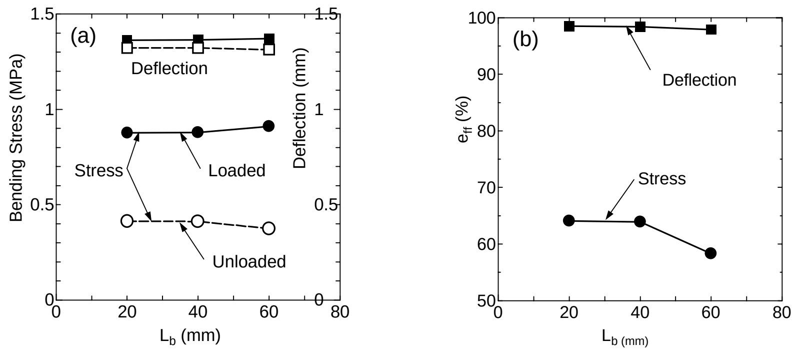

Figure 20 Effect of L_b on (a) Stress and Deflection and (b) Load Transfer Efficiencies.

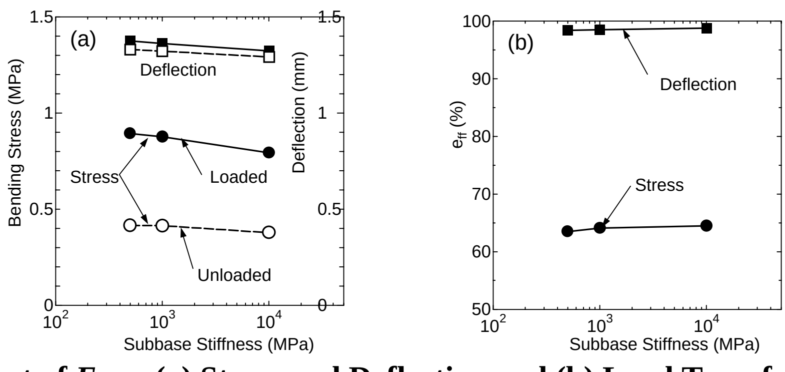

Figure 21 Effect of E_b on (a) Stress and Deflection and (b) Load Transfer Efficiencies.